Effect of rapeseed oil on the rheological, mechanical and thermal properties of plastic lubricants

Effect of rapeseed oil on the rheological, mechanical and thermal properties of plastic lubricants

Lubomír Lapčík[1,2], Martin Vašina[3], Barbora Lapčíková[1,2], Adam Bureček[3], Lumír Hružík[3]

[1]Department of Physical Chemistry, Palacky University, Faculty of Science, 17. Listopadu 12, 771 46 Olomouc, Czech Republic

[2]Tomas Bata University in Zlin, Faculty of Technology, Nam. T.G. Masaryka 275, 76Q Q1 Zlin, Czech Republic

[3]Department of Hydromechanics and Hydraulic Equipment, VŠB-Technical University of Ostrava, Faculty of Mechanical Engineering, 17. Listopadu 15/2172, 7Q8 33 Ostrava-Poruba, Czech Republic

Corresponding author - L. Lapcík lapcikl@seznam.cz

Abstract

A strong difference in the physico-chemical properties of the plastic lubricants studied was found in this study through pressure drop, thermal analysis, vibration damping, texture hardness and rheological measurements. Oxidation aging of the lubricant sample containing rapeseed oil additive was proposed. Its higher thermal sensitivity was simultaneously confirmed by frequency dependent complex shear modulus of elasticity measurements as well as by rheological testing. Rapeseed oil modified lubricant showed a higher decrease in both storage and moduli losses due to a temperature increase from 16 to 26 ° C compared to the rapeseed oil free sample. Simultaneously, the flow curves were shifted to the higher shear stresses (for plastic lubricant without rapeseed oil additive) typical for rheopectic fluids. For the rapeseed oil modified lubricant, the flow curves were shifted to the lower shear stresses, indicating its thixotropic fluid behaviour. The synthetic lubricant without rapeseed oil additive exhibited higher dissipative rheological behaviour as reflected by decreasing first resonance frequency peak position compared to the rapeseed oil modified lubricant as obtained from vibration damping measurements. It was found that the synthetic lubricant exhibited better vibration damping properties and mechanical energy dissipation into heat due to its higher viscous friction than the rapeseed oil modified lubricant under experimental conditions.

Keywords: Plastic lubricants, viscous friction, mechanical testing, thermal analysis, rheology

1 Introduction

During motion of functional surfaces of a tribological system, it is necessary to separate functional surfaces of a tribological system by a continuous layer of lubricant. The primary function of the lubricants is to reduce the coefficient of friction so as to enable the contact materials to slip on one another to reduce the wear of the part. (**Ali and Xianjun 2015**). Liquid, plastic (lubricant greases), solid and gas lubricants are used for this purpose (**Wieck-owski and Dyja 2017; Kupcinskas et al. 2012**). Plastic lubricants are an essential category of lubricants for particular application conditions. They remain permanently on sliding surfaces. Plastic lubricants are used for lubrication of sliding contacts (e.g. motor vehicles), roller bearings, water pump bearings, gears, cam, piston rings, transmissions, metals, quick plastic forming etc. (**Hsu and Gates 2005; Krajewski and Morales 2004**). They are applied in central lubricating systems that are used to deliver lubricant to lubricated locations of stationary or

mobile machines and equipment, chassis, superstructures and technological equipment of trucks etc. The lubricant is supplied to a lubricating node at given time intervals, e.g. when lubricating hardly accessible bearings that require lubrication refilling. Roller bearings can also be present in such designs that plastic lubricant capacity is used in the technical lifetime of the bearings. Plastic lubricant is also used at high pressures and temperatures and low sliding velocities, e.g. during boundary lubrication (**Hsu and Gates 2005**). Boundary lubrication is defined as the lubrication regime where the average oil film thickness is less than the composite surface roughness, while the surface asperities come into contact with each other under relative motion. The lubricant is not used for the lubrication of similar sliding assemblies and higher sliding velocities. Plastic lubricant protects a bearing in a dusty, humid or chemically aggressive environment against intrusion of surrounding substances in contrast to mineral oil, the lubricant dissipates mechanical friction by heat generated only in part (**Bečka 1997**). The mechanical dissipation of friction produces heat which, depending on the motion velocity, increases the temperature at the contact asperities substantially to the flash temperature for a microsecond time interval. Therefore, studies have been reported demonstrating the variety of thermally induced chemical reactions, e.g. oxidation of the surfaces and lubricants (**Pu et al. 2015**), lubricant degradation (**Polansky et al. 2017**), surface catalysis, polymerization (**Larsson and Andersson 2000**) and formation of organometallic chemistry (**Hsu and Gates 2005**). The latter mentioned chemical reactions led to the production of various inorganic and organic products of varying molecular masses. That is why the formulation of lubricants requires a careful balancing of various chemistries in order to adapt the lubricant to a specific environment and application conditions for required performance (**Airey et al. 2020**).

Plastic lubricants are multicomponent colloidal systems containing base oil, a thickener, various fillers and additives (**Zaimovskaya et al. 2016**). They are most commonly produced in two phases. The dispersive phase is formed by lubricating oil base of petroleum origin. In the case of ecological lubricants, the dispersive phase is formed by vegetable (e.g. rapeseed oil) or synthetic oils. The liquid component of the lubricant varies from 70 to 90 w.%. The dispersed phase is formed by a thickening agent with a lubricant content varying from 5 to 30 w.%. In general, base oils of the plastic lubricants are categorised by the American Petroleum Institute into five groups, depending on the mineral oil base content of saturates and sulphur (**Airey et al. 2020**). Inorganic substances (bentonite, silica gel), organic polymers (e.g. polyuria and polyamides), pigments, and hydrocarbons (paraffin, waxes) are used as the thickening agents. Sodium, calcium, lithium or combined lubricants are also other recognised lubricants. The thickening agent forms a structural grid in which the oil component is bounded. Plastic lubricants are produced by mixing and boiling lubricating oil with a thickening agent. In order to obtain specific properties, lubricants may contain refining additives, e.g. high-pressure additives, stiff lubricants (graphite, molybdenum disulphide), antioxidants and anti-corrosive agents. The content of the refining additives varies from 0.5 to 5 w.% (**Bečka 1997**).

Lime soaps are characterised by a smooth butter-like structure and a very good water resistance. However, their application is limited to temperatures of up to 70 °C. Soda soaps are not resistant to water compared to lime base plastic lubricants. They are characterised by a good interfacial adhesion and sealing. It is possible to apply these soaps generally to temperatures of 100 °C. Lithium soaps have a similar (i.e. smooth and butter) structure to lime plastic lubricants (**Nevrly and Pavlok 2000**). They combine the advantages of lime and sodium plastic lubricants (i.e. water resistance and higher temperatures of application). Their adhesion to metal surfaces and resistance to high temperatures is very good. They are practically insoluble in water and are widely used in technical practice. Their working temperature range is from -30 to 120 °C. Aluminium soaps have a good water resistance, adhesion and ductility. Their working temperature range is from -15 to 80 °C. In the case of the complex soaps, the hardener is formed by both metallic soap and other substances (i.e. by a different compound

of the same metal). Lime, lithium and aluminium complex lubricants are among the most commonly used lubricants (**Štěpina and Veselý 1992; Bečka 1997**).

At present, the emphasis is also on the application of biodegradable lubricating oils in the industrial lubrication system (**Buczek and Zajezierska 2015; Stanciu 2019**). However, relatively little information is available in the literature on experimental studies of mechanical kneading process on the physico-chemical properties of plastic lubricants. Authors (**Hayashi et al. 2014**) theoretically studied the influence of mechanical kneading on the occurrence of residual stresses during tableting by means of finite element methods (FEM) analysis. That is why this experimental study focussed on the effect of rapeseed oil additive on thermal and rheological properties of commercial lubricants by means of thermal analysis, rotational vis-cometry, a novel vibration damping technique and pressure drop measurements.

2 Experimental materials and methods

2.1 Materials

Two plastic lubricants were studied, i.e. Mogul LV 00-EP (Paramo, Czech Republic) and Madit OHV 000 (VURUP Slovnaft, Slovak Republic). **Table 1** presents detailed description and labelling of samples. Both samples under study were experimentally tested prior and after mechanical loading. After storage at 24 °C, original unkneaded samples were measured without mechanical kneading. Next, the samples labelled as kneaded were subjected to mechanical kneading by circulation of the tested lubricants in a hydraulic circuit for a period of 24 hours prior to the experimental measurements.

Table 1 Samples labelling and their description

Sample	Description
1	Lubricant Mogul LV 00-EP (Paramo, Czech Republic), density at 15 °C = 925 kg/m^3, ignition point over 210 °C, autoignition temperature over 355 °C, yellow brownish colour. Major components composition: paraffinic oils > 80 w.%, lithium hydroxide, 12-hydroxy stearic acid[a].
2	Lubricant Madit OHV 000 (VURUP Slovnaft, Slovak Republic), density at 20 °C = 910 kg/m^3, minimum ignition point 105 °C, autoignition temperature 320 °C, green colour. Major components composition: C_{16}-C_{18} fatty acids > 55 w.%, rapeseed oil > 20 w.%, *n*-alkanes C_{14}-C_{18} > 14 w.%, Baragel 10 > 7 w.%, propylene carbonate > 1 w.%[a].

[a]According to manufacturer's data sheet.

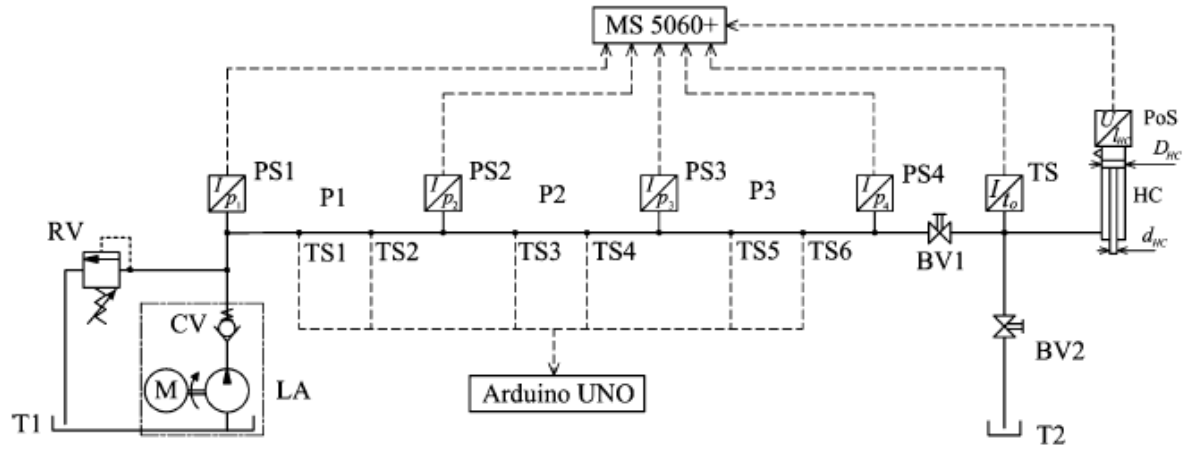

Fig. 1 Schematic representation of the measuring apparatus of pressure drops in the hydraulic system under study

2.2 Pressure drop measurements

Pressure drop measurements were performed at temperatures of 16 and 26 °C. Measurements were realised at different flow rates in steel pipes of 3, 5 and 7 mm inner diameters (d). The schematic diagram of the experimental apparatus is shown in **Fig. 1**. Measuring apparatus consisted of lubrication aggregate (LA), relief valve (RV), steel pipe (P), two ball valves (BV1) and (BV2), two tanks (T1) and (T2), hydraulic cylinder (HC) and sensors. Lubrication aggregate LA (Tribos ACF 02 (TriboTec, Czech Republic)), consisted of an electromotor (EM), piston hydraulic pump (HP) and check valve (CV) (Supplementary materials Fig. S1). The hydraulic pump supplied studied lubricants into the pipe P and the ball valve BV1. Subsequently, the lubricant flowed into the tank T2 either through the ball valve BV2 (Supplementary materials Fig. S2). The latter hydraulic cylinder HC was used to measure the lubricant flow rate. The relief valve RV was used to protect the measuring apparatus against system overload. The steel pipe P with length (l) of 9 m was made up of three steel pipes (P1), (P2) and (P3) of l = 3 m. It was possible to change the lubricant flow rate by varying the hydraulic pump (HP) revolutions through changing the voltage of the electromotor (EM) (ranging from 4 to 24 V, voltage step 2 V) that is firmly fixed to the pump HP. The pressure of the lubricant p was measured at four different points by pressure sensors (PS1) - (PS4) (PR 15 Hydrotechnik, Germany of 0.5 % accuracy). The temperature of the lubricant was measured by temperature sensor (TS) (PT100 Hydrotechnik, Germany of 1% accuracy) (TS1) - (TS6) (DS18820, Dallas Semiconductor, USA) mounted along the pipe P. The lubricant flow rate was determined from the change in HC piston position measured by linear position sensor (PoS) (LTP 150, ATEK Sensor Technologies, Turkey, of 0.3% linearity). Measured data from the sensors PS1 - PS4, TS and PoS were processed by MS 5060 + (Hydrotechnik) unit. Measured temperatures from the temperature sensors TS1-TS6 were recorded by an Arduino UNO-microcontroller (ATmega328) (Atmel, USA). These sensors were connected to the system in order to check the temperature uniformity of the pipe during measurements.

Measurements were performed with the output discharge configuration directed to the hydraulic cylinder and the closed ball valve BV2 (in this case, there were measured time dependences of the piston positions and the mean lubricant flow velocity, pressure gradient in the pipe and the temperature, were subsequently calculated). The time dependences of the pressure p_1 on the sensor PS1 at the beginning of the pipe P1, the pressure p_2 on the sensor PS2 at the pipe end P1, the pressure p_3 on the sensor PS3 at the pipe end P2, the pressure p_4 on the sensor PS4 at the pipe end P3, the lubricant temperature t0 on the sensor TS at the pipe end P3 and the piston position s of the hydraulic cylinder HC on the position sensor PoS, were recorded for individual flow rates. During the lubricant

drainage from the cylinder HC, the ball valve BVi was closed and the ball valve BV2 was opened. Measured data were evaluated using HYDROcomsys/win software (Hydrotechnik) after transferring the data files from the internal memory of the 5060+ Hydrotechnik equipment to the PC.

The pressure drops Δp of the measured pipe were determined as a difference of mean values of the pressure p_1 from the pressure sensor PS1 and the pressure p_4 from the pressure sensor PS4 during the recorder time Δt. Examples of the measured time dependences of the pressure p_1 on the sensor PS1, the pressure p_4 on the sensor PS4 and the piston position during pulsating flow are shown in Supplementary materials Fig. S3. On the basis of the known piston diameter DHC, the piston rod diameter dHC and the piston position change As, the lubricant volume V extruded from the pipe during the time interval At was determined by the equation

$$V = \frac{\pi(D_{HC}^2 - d_{HC}^2)}{4}\Delta S \qquad (1)$$

The mean value of the lubricant volume flow rate QV during the time interval Δt was given by the equation

$$Q_V = \frac{V}{\Delta t} \qquad (2)$$

The mean lubricant flow velocity (u) in the pipe of the inner diameter d was subsequently determined from the formula:

$$u = \frac{4Q_V}{\pi d^2} \qquad (3)$$

The single-phase pressure drop (Δp) was defined as (**Kneer et al. 2018; Warnakulasuriya and Worek 2008; Garcia-Hernando et al. 2009**):

$$\Delta p = \lambda \frac{l}{d}\frac{\rho}{d}u^2 \qquad (4)$$

where λ(−) is the pipe friction coefficient and ρ (kg/m^3) is the lubricant density.

2.3 Thermogravimetry and differential thermal analysis

Thermogravimetry (TG) and differential thermal analysis (DTA) experiments were performed on simultaneous DTA-TG apparatus (Shimadzu DTG 60, Japan). Throughout the experiment, sample weight and heat flow changes vs temperature were continuously monitored. Measurements were

performed at a heat flow rate of 10 °C/min in a dynamic nitrogen atmosphere with a flow rate of 50 ml/min at a temperature range from 35 °C to 550 °C. The samples were then placed in aluminium pans for TG/DTG measurements. An empty aluminium pan was used as a reference and the DTG/DTA was calibrated using indium and zinc. The enthalpy and transition temperatures, known as peak temperatures (T_p), were determined based on the DTA heating curves.

2.4 Dynamic stiffness measurements

The material's ability to damp mechanical vibrations can be described by different quantities. The transfer damping function D (dB) is defined by the equation (**Lapčík et al. 2017a,b**)

$$D = 20 \log \frac{v_1}{v_2} \qquad (5)$$

where v_1 is the velocity amplitude on input (i.e. excitation) side of the tested material, and v_2 is the velocity amplitude on output side of the tested material. The transfer damping function depends on excitation frequency, material thickness, mass load etc. In case of harmonic vibration, it is possible to modify Eq. (**5**) as follows:

$$D = 20 \log \frac{a_1}{a_2} \qquad (6)$$

where α_1 is the acceleration amplitude on input side of the tested material, and α_2 is the acceleration amplitude on output side of the tested material. Mechanical energy damping properties of the studied plastic lubricants were obtained by the forced oscillation method (**Bonfiglio et al. 2016; Lapčík et al. 2018**). The transfer damping function was experimentally measured using vibrator device BK 4810 combined with the three-channel signal multianalyser PULSE BK 3560-B-030 and the power amplifier BK 2706 in the frequency range from 2 to 3200 Hz. Sine oscillations were generated by the vibrator device. The input and output acceleration amplitudes on the input and output sides of the investigated lubricants were recorded by accelerometers BK 4393 (Bruel and Kj$r, Denmark). The D were measured for three different mass loads (28, 112 and 608 g) which were mounted on the upper side of the tested lubricants. Dimensions of the sample vessels were (60 x 60) mm (height x width) and different heights (10, 20 and 30 mm). Each experiment was repeated five times at an ambient temperature of 26 °C.

2.5 Flow curves measurements

Rheological measurements of the studied lubricants were performed on universal laboratory rheometer Brookfield DV-II+Pro (Brookfield, USA). Measuring sensor geometry of cylinder-cylinder was used. Temperature was controlled by Thermostat Brookfield TC-502 (Brookfield, USA). Experimental data of shear stress/or dynamic viscosity vs shear rate dependences were obtained at temperatures of 16 and 26 °C, respectively, with an accuracy of ± 0.5 °C. Experimental data were statistically analysed and fitted by Herschel-Bulkley rheological model (**Hermany et al. 2018; Hammadi et al. 2013**):

$$\tau = \tau_0 + k\dot{\gamma}^n \qquad (7)$$

where k is the consistency coefficient (Pa s^n), n is the flow index (—), τ is the shear stress (Pa), $\dot{\gamma}$ s the shear rate and τ_0 is the yield stress (Pa) (**Lapčíková et al. 2017**).

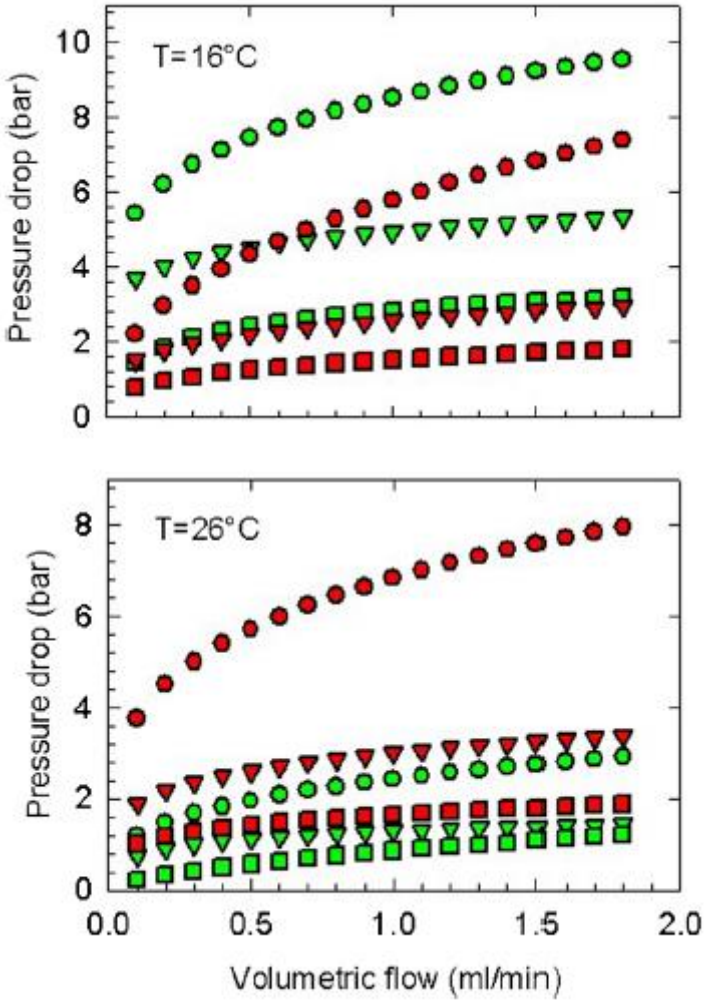

Fig. 2 Pressure drop vs volumetric flow dependencies at 16 and 26 °C for sample 1 (red colour) and sample 2 (green colour) as obtained in different inner cross-section diameters of testing pipes: circle - 3 mm, triangle - 5 mm, square - 7 mm (Color figure online)

2.6 Texture analysis

Lubricant hardness was measured on TA.XTplus texture analyser (Stable Micro Systems, UK). Measurements were performed at 25 ± 1 °C with a cylindrical probe P20 having a diameter of 20 mm, penetration depth of 10 mm, probe speed of 2 mm/s, trigger force of 5 g and strain deformation of 25%. Each sample was measured in triplicate.

2.7 Dynamic mechanical testing

Dynamic oscillatory shear rheometer (Rheostress 1, Haake, Germany) equipped with the plate-plate sensor geometry (of 35 mm diameter and 1 mm gap) was used to determine the viscoelastic properties of the lubricants. All samples were measured in the control shear stress mode at a frequency ranging from 0.01 to 100.00 Hz (at 16 and 26 °C, accuracy of ± 0.1 °C). The amplitude of shear stress (20 Pa) was selected in the linear viscoelasticity region. Storage (O') and loss (G") moduli were determined as a function of excitation frequency f. Individual rheological measurements were repeated four times.

3 Results and discussion

3.1 Pressure drop measurements

Results of the pressure drop measurements are summarised in **Fig. 2**. Here, typical nonlinear patterns were observed for both studied lubricants, suggesting their complex rheological behaviour such as thixotropy and rheopexy.

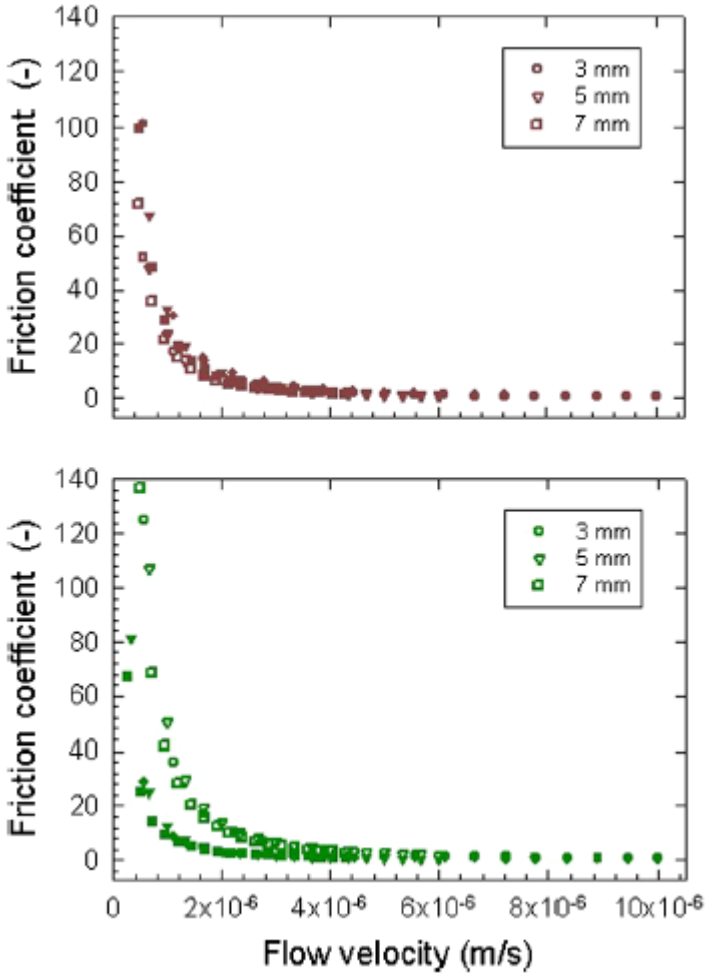

Fig. 3 Friction coefficient vs flow velocity dependences for sample 1 (brown symbols) and sample 2 (green symbols) at 16 °C (empty symbols) and 26 °C (full symbols). Inset legend: inner pipe diameters (Color figure online)

The pressure drop increased with decreasing pipe diameter, as well as with the increasing flow velocity (u), as given by Eq. (**4**) for both samples. This phenomenon is responsible for higher energy dissipation into heat during flow by viscous friction mechanism. However, the difference in rheological behaviour was found for temperature dependent experiments, where the observed pressure drop of the sample 1 increased from 2.22 bar to 3.77 bar (pipe of d = 3 mm and Q_V = 0.1 cm^3/min) with increasing temperature from 16 to 26 °C. On the contrary, increased Δp in sample 2 exhibited a significant decrease in Δp from 5.44 bar to 1.19 bar under the same experimental conditions. The same flow patterns were observed for 5 mm and 7 mm inner pipe diameters as evident in **Fig. 2**. It was observed that the flow in sample 1 was characterised by increasing flow resistivity due to the increasing pressure drop with increasing experimental temperature. On the contrary, sample 2 exhibited decreasing Ap with increasing temperature, suggesting its higher fluidity. Friction coefficient was calculated from the obtained pressure drop and volumetric flow experimental data according to Eq. (**4**), as shown in **Fig. 2**. The flow velocity was calculated according to Eq. (3). It was found that the friction coefficient was exponentially decreasing with increasing flow velocity. Sample 2 was found to be highly sensitive to temperature compared to sample 1. This is clearly visible from **Fig. 3**, where sample 1 friction coefficient dependences were merged in one curve for both experimental temperatures. Contrary to sample 1, a clear difference of the latter X vs u dependences for the experiments was realised at 16 °C and 26 °C for sample 2, by the appearance of clearly distinguished two curves merged from the experimental data obtained for different pipe diameters.

3.2 Rheological measurements

Not surprisingly, due to the shear thinning character of the lubricants tested, as shown in the flow curves shown in **Fig. 4**, the friction coefficient decreased exponentially with an increase in temperature. Hershel-Bulkley rheological model Eq. (**7**) was used to simulate experimental flow curves shown in **Fig. 4**. Results of the non-linear fitting according to the model of Eq. (**7**) are given in **Table 2**. Here, for all measured samples and experimental conditions, the flow index was smaller than 1, indicating pseudoplasticity of the studied lubricants. For sample 1, the parameter n was about 0.4 to 0.6 for both temperatures under study. For sample 2, the parameter n was about 0.2 to 0.5. Both samples exhibited yield stress behaviour as indicated by the observed magnitudes of τ_0. Sample 1 exhibited increase in yield stress after mechanical kneading from 9.5 to 18.1 Pa at 16 °C and from 10.0 to 19.9 Pa at 26 °C. The same trend was also observed for sample 2, where after mechanical kneading the τ_0 was increased from 0.4 to 12.4 Pa at 16 °C and from 5.2 to 8.1 Pa at 26 °C. However, different trends were found for calculated consistency index after kneading; increasing from 28 to 30 Pa s at 16 °C and from 24 to 30 Pa s at 26 °C for the sample 1 in a typical fashion characteristic of rheopectic fluids. In the case of sample 2, this phenomenon was opposite, the index *k* decreased from 44 to 19 Pa s at 16 °C and from 14 to 6 Pa s at 26 °C, indicating thixotropic fluids behaviour. These phenomena were also clearly recognisable by the flow curves shown in **Fig. 4** for the two experimental temperatures. For sample 1, after kneading, the flow curves shifted to higher shear stresses, typical for rheopectic fluids while for sample 2 it shifted to lower shear stresses, indicating thixotropic fluid character. A relatively small hysteresis indicated microstructural homogeneity of the tested lubricants, being highest for sample 1 for both unkneaded and kneaded samples. In the case of sample 2, the hysteresis loop was smaller for both studied temperatures after kneading than the unkneaded sample, indicating higher inhomogeneity character of the original material (**Sha et al. 2016**).

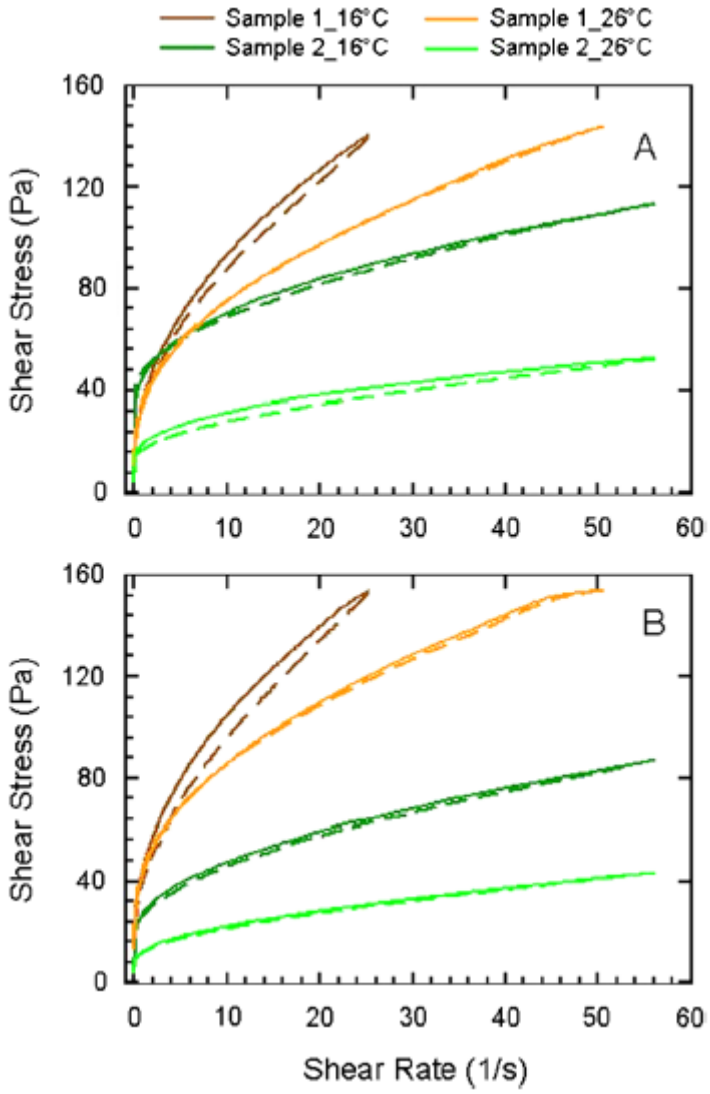

Fig. 4 Shear stress vs. shear rate dependences of the studied lubricants: A - unkneaded samples, B - kneaded samples. For all curves full line -increasing shear rate (up) measurement, dashed line -decreasing shear rate (down) measurement

Table 2 Calculated Herschel - Bulkley flow curve parameters of the tested lubricants at 16 °C and 26 °C measurements temperatures

Sample	Lubricant processing	Shear rate	Lubricant temperature (°C)					
			16			26		
			Flow curve model parameters[a]					
			k (Pa s)	τ_0 (Pa)	n (–)	k (Pa s)	τ_0 (Pa)	n (–)
1	Unkneaded	Increasing	27.9	9.5	0.48	24.3	10.0	0.43
		Decreasing	23.0	12.5	0.52	22.1	14.6	0.45
	Kneaded	Increasing	30.0	16.3	0.47	29.8	13.0	0.40
		Decreasing	21.7	18.1	0.56	25.0	19.9	0.43
2	Unkneaded	Increasing	44.1	0.38	0.22	14.1	5.20	0.29
		Decreasing	36.6	0.97	0.24	8.43	8.05	0.40
	Kneaded	Increasing	19.3	0.70	0.34	5.95	6.19	0.45
		Decreasing	13.2	12.4	0.42	5.16	6.31	0.48

[a]Standard errors: k ± 6%, τ_0 ± 15%, n ± 6%

The frequency dependences of complex shear modulus and its components (G, G") at temperatures of 16 and 26 °C for both studied samples are shown in **Fig. 5**. Sample 1 showed more dissipative character of the mechanical response as indicated by dominating loss modulus (G") than storage modulus (G') at frequencies exceeding 5 Hz for both tested temperatures.

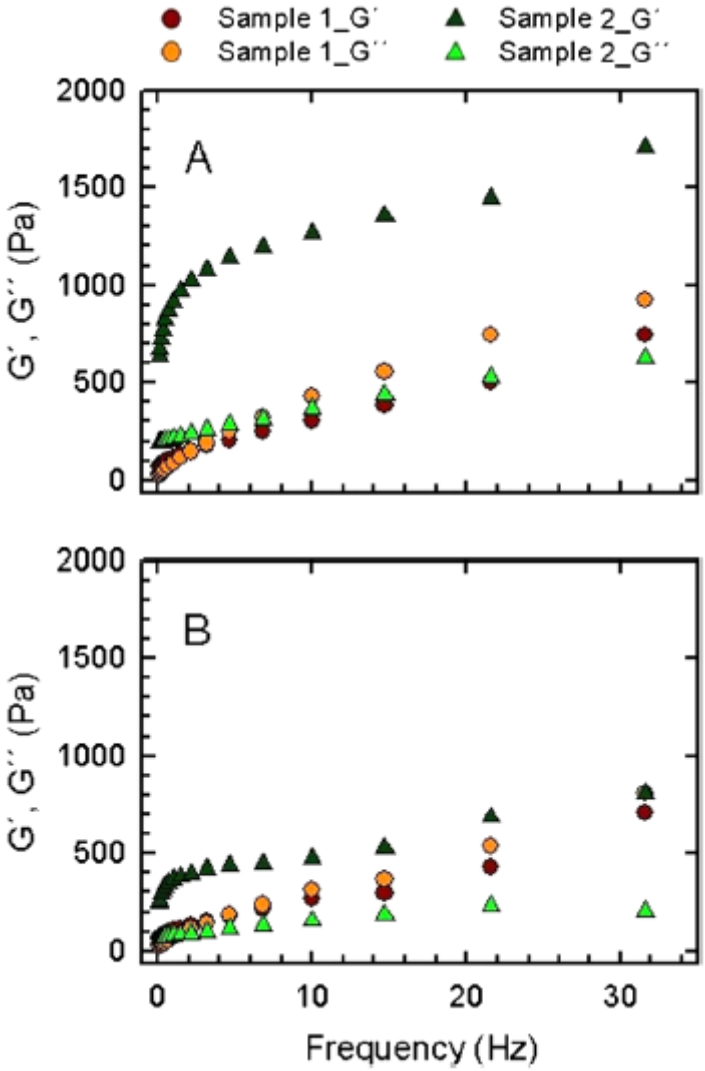

Fig. 5 Frequency dependences of the real and imaginary parts of the complex shear modulus of elasticity of studied materials at 16 °C (A) and 26 °C (B)

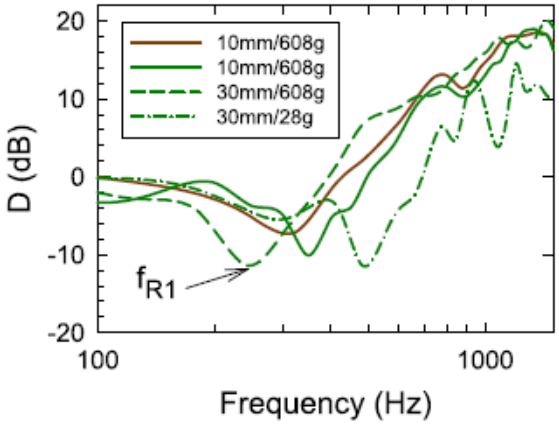

Fig. 6 Frequency dependences of transfer damping function of the tested lubricants: brown line - sample 1, green lines - sample 2. Inset legend: lubricant height (mm)/inertial mass (g). Measurement temperature of 26 °C (Color figure online)

Table 3 First resonance frequency (f_{R1}) and corresponding transfer damping function (D_{R1}) of the studied lubrications as induced by harmonic force vibration

Sample	Height [mm]	Inertial mass [g]					
		28		112		608	
		f_{R1} [Hz]	D_{R1} [dB]	f_{R1} [Hz]	D_{R1} [dB]	f_{R1} [Hz]	D_{R1} [dB]
1	10	677 ± 22	-6.3 ± 0.6	464 ± 21	-6.2 ± 0.4	314 ± 9	-11.0 ± 0.3
	20	567 ± 19	-6.7 ± 0.3	427 ± 16	-8.2 ± 0.6	264 ± 9	-11.8 ± 0.6
	30	446 ± 14	-12.1 ± 0.6	371 ± 11	-11.9 ± 0.5	210 ± 10	-11.2 ± 0.5
2	10	707 ± 21	-7.6 ± 1.0	576 ± 26	-10.5 ± 1.1	387 ± 11	-11.7 ± 0.7
	20	602 ± 27	-12.7 ± 0.8	462 ± 24	-12.0 ± 0.6	316 ± 13	-10.6 ± 0.5
	30	488 ± 15	-11.8 ± 0.7	401 ± 11	-12.1 ± 0.6	264 ± 10	-11.5 ± 0.7

This was contrary to sample 2 which showed the higher elasticity behaviour as reflected by observed higher magnitudes of the storage modulus than the loss modulus in the whole frequency range and both temperatures, thus indicating its higher stiffness. There was an increase in the order of magnitude of the storage modulus compared to the loss modulus for sample 2; this is in comparison to the patterns observed for the sample 1, indicating more gel like character of the lubricant sample 2. Simultaneously, there was higher thermal sensitivity of the sample 2 than the sample 1 as indicated by observed vigorous moduli decrease at 26 °C temperature; this is in comparison to the 16 °C temperature. These findings are in excellent agreement with friction coefficient data presented in **Fig. 3**.

3.3 Vibrations damping experiments

To confirm higher mechanical stiffness of sample 2 than sample 1, frequency dependences of the transfer damping function were measured. As demonstrated in **Fig. 6**, a shift in the typical first resonance frequency peak position to the higher excitation frequency (**Lapčík et al. 2017a,b; Vašina et al. 2019**) was observed for sample 2 (e.g. f_{R1} = 387 Hz for 10 mm sample height and 608 g inertial mass) than for sample 1 (e.g. f_{R1} = 314 Hz for 10 mm sample height and 608 g inertial mass) for all lubricant heights and inertial masses applied (see data in **Table 3**). Sample 1 exhibited higher dissipative behaviour due to the higher internal friction and viscosity, as reflected by decreasing first resonance frequency peak position compared to sample 2, and also by a low hardness of 0.112 N to be compared with 0.131 N as observed for sample 2. That is why sample 1 exhibited better vibration damping properties under all experimental conditions (see data in **Table 3**).

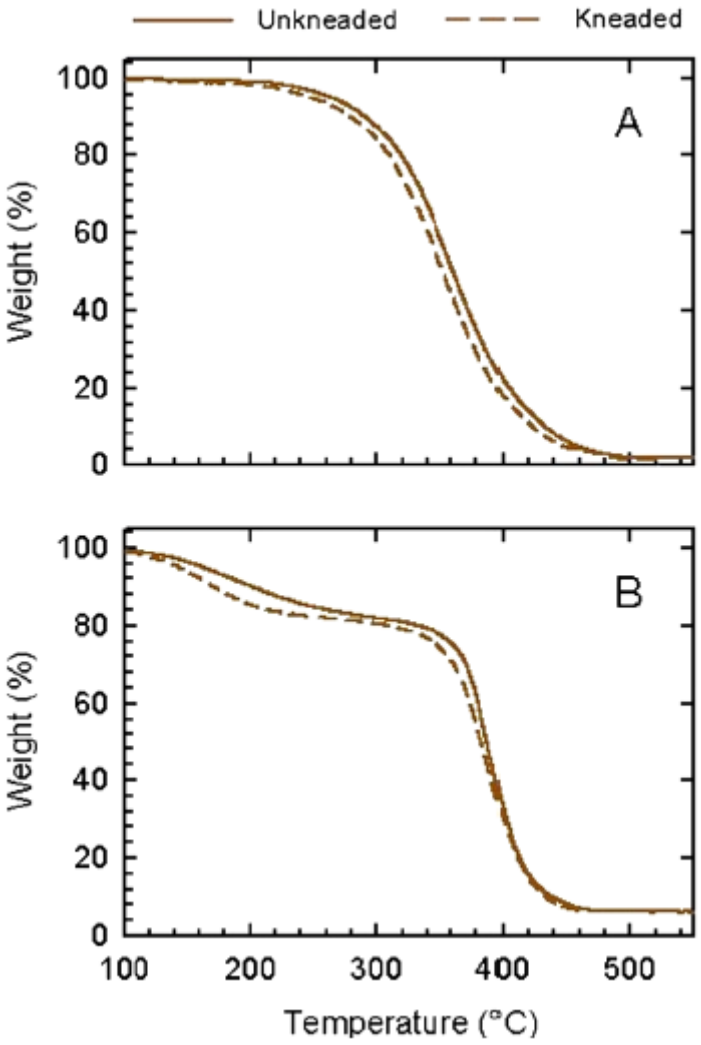

Fig. 7 Results of the thermal gravimetry measurements of the studied lubricants: A - sample 1, B - sample 2

Table 4 Results of the DTA analysis of the studied plastic lubricants

Sample	Lubricant processing	T_{p_1} (°C)	ΔH_1 (J/g)	T_{p_2} (°C)	ΔH_2 (J/g)
1	Unkneaded	202.3	4.7	358.5	239.9
	Kneaded	202.8	6.6	358.3	396.5
2	Unkneaded	181.0	14.1	390.7	124.9
	Kneaded	180.8	22.0	391.0	235.0

3.4 Thermal analysis

Higher temperature sensitivity of friction coefficient of sample 2 than of sample 1 as shown in **Fig. 3** was also experimentally confirmed by thermal analysis as shown in **Figs. 7** and **8** and in **Table 4**. Higher thermal resistance to decomposition processes of the sample 1, as indicated by a constant weight

plateau up to approximately 200 ° C (Fig. 7A), than the observed decrease in sample weight for sample 2 was evident here. It was found that mechanical kneading decreased the stability of both lubricants as reflected by higher weight losses in the entire measured temperature range (**Fig. 7**). As shown in Fig. 7A, sample 1 exhibited two stages decomposition process comprising volatile evaporation at 202 °C and release of carbon containing volatiles at 358 °C; however, sample 2 exhibited three stage decomposition process comprising dehydration and volatile evaporation at 181 °C and 300 °C, followed by release of carbon containing volatiles at 391 °C similar to the observation of **Chen et al. (2017)**.

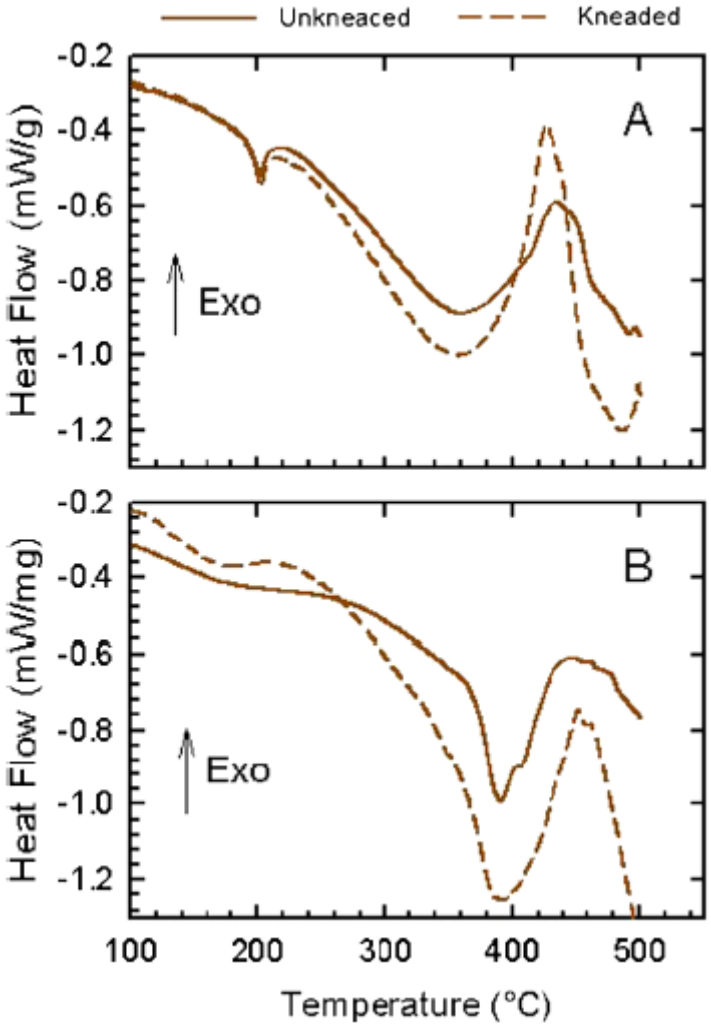

Fig. 8 Results of the differential thermal analysis measurements of the studied lubricants: A -sample 1, B - sample 2

After mechanical kneading, both lubricants exhibited onset of the endothermic peaks at lower temperatures as shown in **Fig. 8**, thus indicating their worse thermal stability. The latter endothermic peaks were ascribed to the evaporation of different fractions of the oil solvent base (**Parajo et al. 2018**). Interestingly, higher evaporation process heats of fusion of both thermal events were observed (sample 1: T_{P1} = 202 °C and T_{p2} = 358 °C, sample 2: T_{p1} = 181 °C and T_{P2} = 391 °C) after kneading originally from 4.7 J/g to 6.6 J/g (peak T_{p1} of the sample 1) and 240 J/g to 397 J/g (peak T_{P2} of the sample 1) and from 14 J/g to 22 J/g (peak T_{P1} of the sample 2) and 125 J/g to 235 J/g (peak T_{P2} of the sample 2),

ascribed to the possible oxidation of the lubricants constituents induced by kneading in ambient air atmosphere (**Chen et al. 2017**).

4 Conclusions

In this study, it was found that the rheological activity of the lubricants tested was different in terms of their temperature sensitivity. Sample 2 modified by rapeseed oil additive was more sensitive to temperature changes than the rapeseed oil free sample 1. These findings were confirmed by means of the pressure drop measurements obtained on cyclic hydraulic piston loading apparatus. This behaviour was attributed to the effect of the different compositions of the plastic lubricants studied. Based on the effect of the kneading process, as induced by the operation of the cyclic hydraulic pump piston during the test, the oxidation aging of the rapeseed oil component in sample 2 was also proposed. Observed higher thermal sensitivity by pressure drop measurements of the rheological behaviour was simultaneously confirmed by the frequency dependent complex shear modulus of elasticity measurements, as well as by the flow curves measurements. Sample 2 contrary to sample 1 exhibited higher decrease in both storage and loss moduli with temperature increase from 16 to 26 °C. Simultaneously, the flow curves shifted to the higher shear stresses for sample 1 typical of rheopectic fluids and for sample 2 it shifted to the lower shear stresses characteristic of thixotropic fluids. Relatively small hysteresis indicated microstructural homogeneity of the tested lubricants. The highest hysteresis was found for sample 1 for both unkneaded and kneaded samples. In the case of sample 2, the hysteresis loop was smaller at both 16 and 26 °C temperatures after kneading than the unkneaded sample, thus indicating higher inhomogeneity structure of the original material. Thermal analysis showed two-stage decomposition process for sample 2 to be compared to the single stage decomposition process observed for sample 1. Here, the first weight loss obtained for sample 2 at 181 °C was attributed to the oxidation process of the lubricant's constituents accompanied by the evaporation of the volatile components and dehydration. Sample 2 exhibited higher mechanical stiffness than sample 1 at 26 °C as observed by the frequency dependences of the transfer damping function measurements. This phenomenon was simultaneously confirmed by the lower pressure drops obtained to be compared to sample 1 that exhibited higher viscous friction. For this reason, sample 1 exhibited higher dissipative rheological behaviour, as reflected by the decreasing first resonance frequency peak position, than sample 2. Therefore, sample 1 exhibited better vibration damping properties at given experimental conditions than sample 2.

References

Airey, J., Spencer, M., Greenwood, R., Simmons, M.: The effect of gas turbine lubricant base oil molecular structure on friction. Tribol. Int. 146, 106052 (2020). **https://doi.org/10.1016/j.triboint.2019.106052**

Ali, M.K.A., Xianjun, H.: Improving the tribological behavior of internal combustion engines via the addition of nanoparticles to engine oils. Nanotechnol. Rev. 4(4), 347-358 (2015). **https://doi.org/10.1515/ntrev-2015-0031**

Bečka, J.: Tribologie. CVUT, Prague (1997)

Bonfiglio, P., Pompoli, F., Horoshenkov, K.V., Rahim, M.I.B.S.A.: A simplified transfer matrix approach for the determination of the complex modulus of viscoelastic materials. Polym. Test. 53, 180-187 (2016). **https://doi.org/10.1016/j.polymertesting.2016.05.006**

Buczek, B., Zajezierska, A.: Biodegradable lubricating greases containing used frying oil as additives. Ind. Lubr. Tribol. 67(4), 315-319 (2015). **https://doi.org/10.1108/ILT-07-2013-0082**

Chen, J., Wang, Y., Lang, X., Ren, X., Fan, S.:Comparative evaluation of thermal oxidative decomposition for oil-plant residues via thermogravimetric analysis: thermal conversion characteristics, kinetics, and thermodynamics. Bioresour. Technol. 243, 37-46 (2017). **https://doi.org/10.1016/j.biortech.2017.06.033**

Garcia-Hernando, N., Acosta-Iborra, A., Ruiz-Rivas, U., Izquierdo, M.: Experimental investigation of fluid flow and heat transfer in a single-phase liquid flow micro-heat exchanger. Int. J. Heat Mass Transf. 52(23-24), 5433-5446 (2009). **https://doi.org/10.1016/j.ijheatmasstransfer.2009.06.034**

Hammadi, L., Ponton, A., Belhadri, M.: Temperature effect on shear flow and thixotropic behavior of residual sludgefromwastewatertreatmentplant. Mech. Time-Depend. Mater. 17(3), 401-412 (2013). **https://doi. org/10.1007/s11043-012-9191-z**

Hayashi, Y., Otoguro, S., Miura, T., Onuki, Y, Obata, Y., Takayama, K.: Effect of process variables on the Drucker-Prager cap model and residual stress distribution of tablets estimated by the finite element method. Chem. Pharm. Bull. 62(11), 1062-1072 (2014). **https://doi.org/10.1248/cpb.c14-00190**

Hermany, L., Lorenzini, G., Klein, R.J., Zinani, F.F., dos Santos, E.D., Isoldi, L.A., Rocha, L.A.O.: Constructal design applied to elliptic tubes in convective heat transfer cross-flow of viscoplastic fluids. Int. J. HeatMass Transf. 116, 1054-1063 (2018). **https://doi.org/10.1016/j.ijheatmasstransfer.2017.09.108**

Hsu, S.M., Gates, R.S.: Boundary lubricating films: formation and lubrication mechanism. Tribol. Int. 38(3), 305-312 (2005). **https://doi.org/10.1016/j.triboint.2004.08.021**

Kneer, A., Wirtz, M., Laufer, T., Nestler, B., Barbe, S.: Experimental investigations on pressure loss and heat transfer of two-phase carbon dioxide flow in a horizontal circular pipe of 0.4 mm diameter. Int. J. Heat Mass Transf. 119, 828-840 (2018). **https://doi.org/10.1016/j.ijheatmasstransfer.2017.11.146**

Krajewski, P.E., Morales, A.T.: Tribological issues during quick plastic forming. J. Mater. Eng. Perform. 13(6), 700-709 (2004). **https://doi.org/10.1361/10599490421330**

Kupcinskas, A., Kreivaitis, R., Padgurskas, J., Makareviciene, V., Gumbyte, M.: Modification of rapeseed oil and lard by monoglycerides and free fatty acids. Mechanika 18(1), 113-118 (2012). **https://doi.org/10. 5755/j01.mech.18.1.1292**

Lapčík, L., Vašina, M., Lapčíková, B., Plšková, M., Gál, R., Brychtová, M.: Application of a vibration damping technique in characterizing mechanical properties of chicken meat batters modified with amaranth. J. Food Meas. Charact. 11(4), 1987-1994 (2017a). **https://doi.org/10.1007/s11694-017-9581-7**

Lapčík, L., Maňas, D., Vašina, M., Lapčíková, B., Řezníček, M., Zádrapa, P.: High density poly(ethylene)/ CaCO3 hollow spheres composites for technical applications. Composites, Part B, Eng. 113, 218-224 (2017b). **https://doi.org/10.1016/jxompositesb.2017.01.025**

Lapcik, L., Manas, D., Lapcikova, B., Vasina, M., Stanek, M., Cepe, K., Vlcek, J., Waters, K.E., Greenwood, R.W., Rowson, N.A.: Effect of filler particle shape on plastic-elastic mechanical behavior of high density poly(ethylene)/mica and poly(ethylene)/wollastonite composites. Composites, Part B, Eng. 141, 92-99 (2018). **https://doi.org/10.1016/jxompositesb.2017.12.035**

Lapcikova, B., Valenta, T., Lapcik, L.: Rheological properties of food hydrocolloids based on polysaccharides. J. Polym. Mater. 34(3), 631-645 (2017)

Larsson, R., Andersson, O.: Lubricant thermal conductivity and heat capacity under high pressure. Proc. Inst.

Mech. Eng., Part J J. Eng. Tribol. 214(J4), 337-342 (2000). **https://doi.org/10.1243/1350650001543223**

Nevrly, J., Pavlok, B. (eds.): Design Methodology of Branched Lubricating Cirquits by Support of the Modern Numerical Systems. Research Report VUT-EU-QR-02-00 (2000)

Parajo, J.J., Villanueva, M., Otero, I., Fernandez, J., Salgado, J.: Thermal stability of aprotic ionic liquids as potential lubricants. Comparison with synthetic oil bases. J. Chem. Thermodyn. 116, 185-196 (2018). **https://doi.org/10.1016/joct.2017.09.010**

Polansky, R., Prosr, P., Vik, R., Moravcova, D., Pihera, J.: Comparison of the mineral oil lifetime estimates obtained by differential scanning calorimetry, infrared spectroscopy, and dielectric dissipation factor measurements. Thermochim. Acta 647, 86-93 (2017). **https://doi.org/10.1016Zj.tca.2016.12.002**

Pu, W., Pang, S., Jia, H.: Using DSC/TG/DTA techniques to re-evaluate the effect of clays on crude oil oxidation kinetics. J. Pet. Sci. Eng. 134, 123-130 (2015). **https://doi.org/10.1016/j.petrol.2015.07.014**

Sha, J., Zhang, F., Zhang, H.: Thixotropic flow behaviour in chemical pulp fibre suspensions. BioResources 11(2), 3481-3493 (2016)

Stanciu, I.: Studies concerning vegetable oils udes as biodegradable lubricant. J. Sci. Arts (1), 195-200 (2019)

Štepina, V., Veselý, V.: Lubricants and Special Fluids. Elsevier, New York (1992)

Vašina, M., Poschl, M., Hružík, L., Bureček, A., Kotrasová, K., Kormaníková, E.: Mechanical properties of rubber composite materials filled with nanofillers. Int. J. Mod. Manuf. Technol. 11(3), 143-150 (2019)

Warnakulasuriya, F.S.K., Worek, W.M.: Heat transfer and pressure drop properties of high viscous solutions in plate heat exchangers. Int. J. Heat Mass Transf. 51(1-2), 52-67 (2008). **https://doi.org/10.1016/). ijheatmasstransfer.2007.04.054**

Wieckowski, W., Dyja, K.: The effect of the use of technological lubricants based on vegetable oils on the process of titanium sheet metal forming. Arch. Metall. Mater. 62(2), 489-494 (2017). **https://doi.org/ 10.1515/amm-2017-0070**

Zaimovskaya, T.A., Bordubanova, E.G., L'yadov, A.S., Parenago, O.P.: Tribological properties of plastic lubricants infused with molybdenum-containing additives. Chem. Technol. Fuels Oils 52(4), 369-376 (2016). **https://doi.org/10.1007/s10553-016-0717-y**